Stable, efficient diode-pumped femtosecond Yb:KGW laser through optimization of energy density on SESAM

Jinfeng Li (李进峰), Xiaoyan Liang (梁晓燕)*, Jinping He (何晋平), and Hua Lin (林 华)

Shanghai Institute of Optics and Fine Mechanics, Chinese Academy of Sciences, Shanghai 201800, China

**Corresponding author: liangxy@mail.siom.ac.cn*

Received September 15, 2010; accepted January 28, 2011; posted online May 26, 2011

An efficient high-power diode-pumped femtosecond Yb:KGW laser is repored. Through optimization of energy density by semiconductor saturable absorber mirror, output power achieved 2.4 W with pulse duration of 350 fs and repetition rate of 53 MHz at a pump power of 12.5 W, corresponding to an optical-to-optical efficiency of 19.2%. We believe that it is the highest optical-to-optical efficiency for single-diode-pumped bulk Yb:KGW femtosecond lasers to date.

OCIS codes: 140.3580, 140.3615, 140.4050, 140.7090.

doi: 10.3788/COL201109.071406.

Diode-pumped solid-state ultrafast laser sources have wide applications in many fields, such as in nonlinear frequency conversion, high-resolution spectroscopy, nonlinear microscopy, and others[1−3]. For a number of applications, having femtosecond lasers with high average output power is desirable, preferably without the use of additional amplifier, which would increase the complexity and manufacturing cost of the whole system. Such lasers can be used to operate relatively simple and efficient nonlinear conversion stages, driving applications such as large-scale displays in red, green, and blue output beams, where several watts of average power are needed[4].

In the past few years, a number of interesting results[5−10] have shown that Yb^{3+}-doped solid-state laser materials are very attractive for the development of diode-pumped femtosecond mode-locked oscillators. This is because of the amazing crystalline characteristics of such oscillators, including low intrinsic quantum defect, elimination of upconversion, excited-state absorption, cross-relaxation, and concentration quenching. Furthermore, among these good properties, the elimination of concentration quenching allows a high doping level and, consequently, a short pump-absorption length. This lowers the demands on beam quality of high-power laser diodes used for pumping, making it very attractive for directly diode-pumped bulk crystalline lasers. The low intrinsic quantum defect also results in an efficient lasing, which makes it suitable for high-efficiency mode-locked lasers.

In all kinds of Yb^{3+}-doped solid-state laser materials, Yb^{3+}:$KGd(WO_4)_2$ (Yb:KGW) is among the most promising because Yb:KGW crystals have broad gain bandwidths (24 nm), high-emission cross-sections (2.8×10^{-20} cm^2), and good thermal conductivity (3.3 $W\cdot m^{-1}\cdot K^{-1}$)[11]. Hence, Yb:KGW femtosecond laser has recently become one of the popular areas in the ultrafast lasers[12−17]. The results of single diode-pumped bulk Yb:KGW femtosecond lasers with the best performance obtained in terms of average output power are summarized in Table 1. The highest power obtained was 3.7 W with a pump power of 22.8 W, corresponding to an optical-to-optical efficiency of 16%[13].

In this letter, an efficient, high-average-power single-diode-pumped Yb:KGW femtosecond laser is reported. On optimizing the energy density by semiconductor saturable absorber mirror (SESAM), pulses as short as 350 fs and an average output power of 2.4 W with a pump power of 12.5 W were achieved, corresponding to an optical-to-optical efficiency of 19.2%. To our knowledge, this is the highest optical-to-optical efficiency for single-diode-pumped bulk Yb:KGW femtosecond lasers thus far.

Figure 1 shows the experimental setup of our diode pumped femtosecond Yb:KGW laser. A fiber-coupled diode laser was used as the pump source, with core-diameter of 200 μm and numerical aperture (NA) of 0.22, emitting at a wavelength of 978 nm at room temperature. A series of lenses with an image ratio of 1:1 was used to focus the pump beam onto the crystal. A classical Z-type cavity containing a dichroic mirror M_1, which has high reflectivity for laser light and high transmission for pump light, was used. Two highly reflective concave mirrors M_2 and M_3, both with radii of curvature of 500, and a plane output coupler were also used. The flat/flat, 3-mm-long, antireflection coated, and 5 at.-% Yb:KGW crystal was wrapped with indium foil and mounted in a water-cooled copper block. Water temperature was maintained at 14°C. A SESAM with saturation fluence of 70 $\mu J/cm^2$, relaxation time of 500 fs, and a maximum modulation depth of 1.2% at one end of the cavity was used to initiate and stabilize the continuous-wave (CW) mode-locking pulse train. The cavity was designed to provide a mode size radius of 90 μm inside the crystal. The round trip cavity length was approximately 2.8 m, giving a pulse frequency of 53 MHz.

Table 1. Summary of the Results for Single-Diode-Pumped Bulk Yb:KGW Femtosecond Lasers

Average Output Power (W)	1.5	2.1	2.3	3.7
Pump Power (W)	11.0	18.0	18.0	22.8
Pulse Width (fs)	260	210	420	296
Optical-to-Optical Efficiency	13.6%	11.7%	13.0%	16.0%
Ref.	[14]	[15]	[16]	[13]

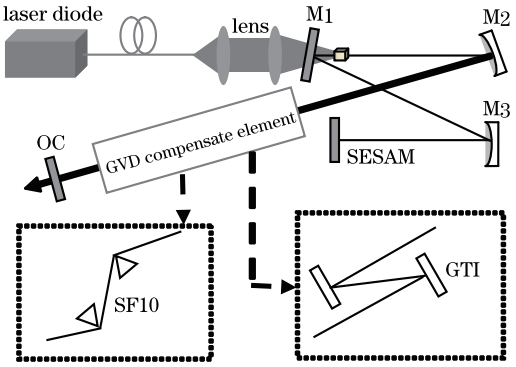

Fig. 1. Schematic setup of CW mode-locked Yb:KGW laser.

As shown in Fig. 1, to introduce the negative group delay dispersion involved in the soliton mode-locking regime, a pair of SF10 prisms and a Gires-Tournois interferometer (GTI) mirror were successively used. This compensated for the positive dispersion within the laser cavity and balanced the self-phase modulation introduced by the Kerr nonlinearity of the laser crystal.

The CW performance, using the cavity shown in Fig. 1, but without any group velocity dispersion (GVD) compensating element and SESAM in the cavity, was first measured. At an absorbed pump power of 10.3 W, the maximum output power of 1.98 W at 1,047.9 nm was obtained with an output coupler (OC) of 1%, corresponding to a laser slope efficiency of 27.5%.

In the mode-locked operation, a pair of SF10 prisms separated by 60 cm were first inserted into the output arm as the compensation element. A SESAM was used to replace the highly reflective mirror at the other end of the cavity. At an absorbed pump power of 8.5 W, an average output power of 200 mW (1% OC) with pulse duration as short as 250 fs can be obtained. The pulse spectrum has a full-width at half-maximum (FWHM) of 5 nm, centered at a wavelength of 1,040 nm. The time-bandwidth product was 0.35, relatively closing to the theoretical value of 0.315 for a sech^2 pulse shape. The autocorrelation trace and pulse spectra are shown in Fig. 2(a). However, because of the high insertion loss of the prism pairs, the output power is very low compared with the CW operation. Hence, a Gires-Tournois interferometer (GTI) mirror providing –2,000-fs^2 GVD with single reflection was used to replace the prism pairs for dispersion compensation to improve output efficiency.

Using only one GTI mirror, the shortest pulse width of 350 fs was achieved with one bounce on the GTI mirror. The maximum output power obtained was 2.4 W at a pump power of 12.5 W with a 9% OC, corresponding to a slope efficiency of 36% and an optical-to-optical efficiency of 19.2% (Fig. 3). The pulse spectrum had a FWHM of 7.8 nm, centered at a wavelength of 1,036 nm. The corresponding autocorrelation trace and pulse spectra are shown in Fig. 2(b). The time-bandwidth product was 0.76, which is 2.4 times larger than the transform-limited value. This indicates that there was still uncompensated higher order dispersion in the cavity and the pulse duration could be further narrowed.

As shown in Fig. 3, the pulse duration became shorter with increasing the output power. This trend is normal for soliton mode-locked lasers, as described in Ref. [19].

In soliton mode-locked regime, the stability of mode-locking is affected by many factors, such as the balance of self-phase modulation and intracavity negative dispersion, energy density on the SESAM, and others. Generally, insufficient dispersion compensation leads to pulse splitting[18]. However, oversaturation of SESAM could also lead to multiple pulsing, which is one of the primary constraints on achieving high average output power in femtosecond mode-locked lasers. Paschotta *et al.* have shown that, under conditions of strong saturation, especially when the saturation parameter is larger than 10, the SESAM could exhibit many additional effects. Such effects are two-photon absorption, free-carrier absorption, thermal effects, or various damages[19].

We also studied the influence of the energy density of SESAM on mode-locked stability. Three cavities were designed with the same type, albeit different cavity parameters, to provide a mode size radii of 50, 110, and 200 μm on the SESAM, respectively. Table 2 shows the results in terms of intracavity energy for different laser work stages.

As shown in Table 2, mode-locking is found to self-start at relatively high intracavity energy E_s. However once

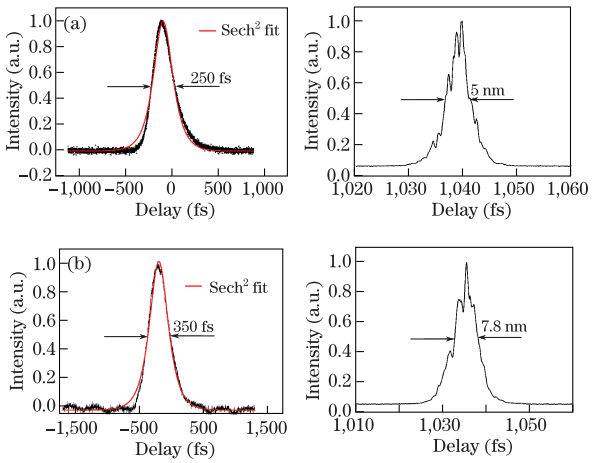

Fig. 2. Autocorrelation trace (left) and pulse (right) spectra of the Yb:KGW laser. (a) Pulse duration of 250 fs with a 5-nm broad spectrum and (b) pulse duration of 350 fs with a 7.8-nm broad spectrum.

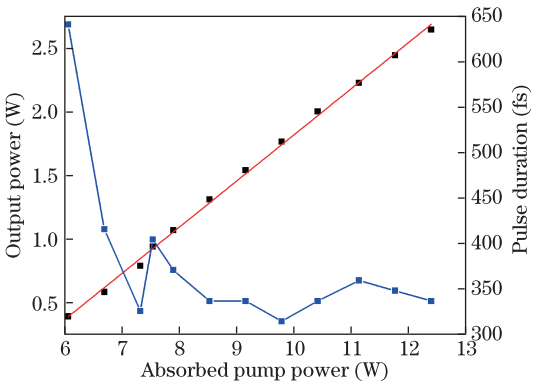

Fig. 3. Dependence of the output power and pulse duration versus absorbed pump power in CWML operation with 9% OC.

Table 2. Results in Terms of Intracavity Energy for Different Laser Work Stages

ω_a (μm)	E_e (nJ)	E_s (nJ)	E_m (nJ)
50	62.9	86.0	206.9
110	104.8	188.7	503.1

ω_a is the beam radius on the SESAM; E_e is the experimental threshold energy for mode-locking; E_s is the energy value for mode-locking self-started; E_m is the energy value for multiple pulsing.

initiated, mode-locking can continue at a smaller value E_e when the pump power decreases. Hence, E_e was taken as the experimental threshold energy for mode locking. Table 2 shows that the energy for mode-locking self-started E_s is 1.4 times the experimental threshold energy E_e with beam radius of 50 μm on the SESAM, and 1.8 times with beam radius of 110 μm on the SESAM.

The energy for multiple pulsing E_m is 3.3 times that of E_e with beam radius of 50 μm on the SESAM and 4.8 times with beam radius of 110 μm on the SESAM. This means when the intracavity pulse energy is 3–5 times that of the threshold, the pulse becomes unstable and breaks up into multiple pulses. However, in the case of beam radius of 50 μm on the SESAM, there is a relatively small beam cross-section. Thus, the E_m of 206.9 nJ, which corresponds to an output power of 987 mW with 9% OC, was calculated to have an energy density of 2,630 μJ/cm^2 on the SESAM. This is 37 times that of the saturation fluence of SESAM. Severe oversaturation leads to unstable mode-locking. Moreover, the SESAM is easily damaged when there are some disturbances on the cavity. In the case of beam radius of 110 μm on the SESAM, E_m of 503.1 nJ, corresponding to an output power of 2.4 W, was calculated to have an energy density of 1,324 μJ/cm^2. No damage on the device was observed. We also tried a cavity that provides a beam radius of 200 μm on the SESAM. However, with 9% OC, obtaining CWML was difficult because of the high threshold. Thus, selecting a suitable beam size on the SESAM is very important for soliton mode-locked lasers. Too-small beam size on the SESAM would lead to very fast oversaturation when increasing pump power and constrain output power; a too-large beam size on the SESAM would make it hard to fulfill the threshold.

In conclusion, we demonstrate a high average output power diode-pumped Yb:KGW femtosecond laser. Pulse duration as short as 350 fs and output power as high as 2.4 W can be achieved with a pumped power of 12.5 W. The corresponding optical-to-optical efficiency is 19.2%. Through more precise dispersion compensation and optimized SESAM parameter selection, shorter pulses and higher output power would be obtained in further work.

This work was supported by the National Science Foundation of China under Grant No. 60921004.

References

1. A. Major, V. Barzda, P. A. E. Piunno, S. Musikhin, and U. J. Krull, Proc. SPIE **5969,** 59690Q-1 (2005).
2. P. Xu, E. Kable, C. J. R. Sheppard, and G. Cox, Chin. Opt. Lett. **8,** 213 (2010).
3. Q. Liu, J. Chen, S. Zhuo, X. Jiang, and K. Lu, Chin. Opt. Lett. **7,** 240 (2009).
4. R. Paschotta, E. Brunner, E. Innerhofer, T. Siidmeyer, and U. Keller, Advan. Solid-State Lasers **68,** 117 (2002).
5. F. Thibault, D. Pelenc, F. Druon, Y. Zaouter, M. Jacquemet, and P. Georges, Opt. Lett. **31,** 1555 (2006).
6. F. Druon, S. Chénais, P. Raybaut, F. Balembois, P. Georges, R. Gaumé, G. Aka, B. Viana S. Mohr, and D. Kopf, Opt. Lett. **27,** 197 (2002).
7. A. Lucca, G. Debourg, M. Jacquemet, F. Druon, F. Balembois, P. Georges, P. Camy, J. L. Doualan, and R. Moncorgé, Opt. Lett. **29,** 2767 (2004).
8. H. Liu, J. Nees, and G. Mourou, Opt. Lett. **26**, 1723 (2001).
9. C. Hönninger, G. Zhang, U. Keller, and A. Giesen, Opt. Lett. **20,** 2402 (1995).
10. W. Li, Q. Hao, H. Zhai, H. Zeng, W. Lu, G. Zhao, L. Zheng, L. Su, and J. Xu, Opt. Express **15,** 2354 (2007).
11. F. Druon, J. Boudeile, Y. Zaouter, M. Hanna, F. Balembois, P. Georges, J. Petit, P. Golner, and B. Viana, Proc. SPIE **6400,** 64000D-1 (2006).
12. G. Paunescu, J. Hein, and R. Sauerbrey, Appl. Phys. B **79,** 555 (2004).
13. A. Major, R. Cisek, and V. Barzda, Opt. Express **14,** 12163 (2006).
14. A. Courjaud, N. Deguil, and F. Salin, in *Proceedings of 2002 Technical Digest* 161 (2002).
15. A. Major, R. Cisek, D. Sandkuijl, and V. Barzda, Laser Phys. Lett. **6,** 272 (2009).
16. A. Major, R. Cisek, and V. Barzda, Proc. SPIE **6108,** 61080Y-1 (2006).
17. G. R. Holtom, Opt. Lett. **31,** 2179 (2006).
18. F. X. Kärtner, I. D. Jung, and U. Keller, IEEE J. Sel. Top. Quantum Electron. **2,** 540 (1996).
19. R. Paschotta and U. Keller, Appl. Phys. B **73,** 653 (2001).